Manuskripteingang: 12. 5. 87

AKADEMIE DER WISSENSCHAFTEN DER DDR
ZENTRALINSTITUT FÜR ELEKTRONENPHYSIK
1086 Berlin, Hausvogteiplatz 5–7

Ag 521/601/87

ZIE

Akademie der Wissenschaften der DDR
Zentralinstitut für Elektronenphysik

Preprint 87-4

STUDIES OF IMPURITY INJEKTION INTO A TOKAMAK PLASMA

D. Hildebrandt,
B. Jüttner,
H. Pursch,
K. Jakubka,
J. Stöckel,
F. Zacek

Mai 1987

STUDIES OF IMPURITY INJECTION INTO A TOKAMAK PLASMA

Dieter Hildebrandt, Burkhard Jüttner and Heinz Pursch

Central Institute of Electron Physics of the Academy of Sciences of the GDR, Berlin, 1086

Karel Jakubka, Jan Stöckel and František Záček

Institute of Plasma Physics of the Czechoslovak Academy of Sciences, 18069 Prague

Abstract

Controlled metal impurity injection into the plasma of the CASTOR-Tokamak has been performed by arc ignition in a special arc source, and by erosion probes exposed to the edge plasma. The injected impurities were Ta and Li. Using standard diagnostics, time resolved photography, collector probes and post-mortem investigations of limiters, the plasma response on the impurity injection and general features of the toroidal flow of the plasma and the impurities have been studied. There are indications of toroidal inhomogeneities of the edge plasma caused by the local impurity injection, and also evidence of nonsymmetrical flow of the plasma and the impurities. Typical directions of the asymmetric component of particle and heat fluxes have been determined in the core, boundary and scrape-off plasma.

1. Introduction

Since the effects of impurities on the performance of tokamaks have been recognized as a serious problem, the production and the behaviour of the impurities are investigated in more detail /1/. There are several approaches to search for natural impurity sources and to study the impurity transport in the core and edge plasma. Besides spectroscopic identification of the impurity species in the core plasma, and in recent time also in the edge plasma, mainly surface analysis of solids after their exposure to the edge plasma have been applied.

Post-mortem investigations of replaced parts of tokamaks proved to give useful information on phenomena of impurity erosion and deposition. However, they are hardly suited to obtain detailed information on plasma effects and impurity transport, because of their long term operation and consequently the superposition of different discharge and cleaning regimes. Collector probe measurements can yield data on actual impurity fluxes in the scrape-off plasma of single discharges. But here problems still arise from the fact that generally the sources of the impurities can be hardly localized. In connection with this the shielding action of the edge plasma cannot be sufficiently investigated. Therefore, up to now, it was difficult to obtain a correlation of impurity fluxes in the scrape-off layer to the central plasma behaviour.

In order to overcome these difficulties a well defined source of impurities which are not inherently present in the tokamak would be desirable. Collector probe measurements in connection with impurity pellet injection carried out in T-10 recently /2, 3/, have shown some characteristic features of impurity fluxes in the core and edge plasma.

In this paper first results of injection experiments at the CASTOR-tokamak are presented. Aims of the experiments were the observation of the plasma response on local, strong impurity injection and investigations of general features of

the impurity transport.

The impurities were injected by controlled metal release in a special arc source near the wall and by plasma erosion of evaporated layers on probes which were exposed to the edge plasma.

Properties of the impurity transport have been examined by photography and collector probes. Furthermore, various limiters, installed only during the period of the injection experiments were investigated post-mortem by surface analysis. The plasma response was detected by standard diagnostics, and also by collector probes.

2. Experimental details

2.1. The tokamak

CASTOR is a small tokamak with a major radius of 0.4 m, and minor radii of the first wall of 0.105 m and of the limiters of 0.080 - 0.085 m, respectively /4/. Discharges with plasma currents of I_p up to 30 kA and a pulse length of about 9 ms at a toroidal field $B_T \leq 2.0$ T can be performed. The plasma parameters are line averaged electron density $\bar{n}_e = 0{,}7 - 2.0 \cdot 10^{19}$ m^{-3}, central electron and ion temperature $T_e(o) = 150 - 300$ eV and $T_i(o) = 50 - 100$ eV, respectively. Intrinsic metallic impurities of CASTOR are the stainless steel components (Fe, Cr, Ni and small amounts of Ti) and Mo as limiter material.

2.2. The arcing and erosion probes

In the present experiment Ta (arcing source) as well as Li and Ag (erosion probe) have been used as nonintrinsic impurities.

The arc plasma source /5/ has a coaxial construction with a central cathode rod of Ta and an anode cylinder of Cu (see fig. 1a). An arc with a current of some kA and a duration of about 0.5 ms was ignited during the stable phase of the tokamak discharge using a trigger voltage of some kV. A scheme of the electrical circuit is shown in fig. 1b. Fig. 2 shows

the characteristics of an arc without applying a magnetic field. The capacity of the arc circuit was chosen such that about 10^{17} Ta-atoms were released from the cathode. It was verified /5/ that about $4 \cdot 10^{16}$ Ta-atoms left the source and could reach the plasma. Unfortunately, the fraction of vapour and of macroparticles of the emitted material was not well defined and could be only estimated roughly. The predominant part of the emitted Ta-droplets had a size of about 1 μm. The erosion probe consists of a Ti- or Ta-plate (about 1 cm^2). One side of this plate was covered with a vapour deposited Li-layer while the other side was covered with a silver layer. The thickness of these layers was 500 nm.

2.3. Experimental configuration

The experiments were carried out with two different configurations (A and B) which are shown in fig. 3. All probes were installed on the top side of the torus. In case A, the arcing source and the erosion probes were located 28 cm from the collector probe in the plasma current direction and faced its electron drift side. The limiters were an aperture limiter and a sector limiter on the torus top side. The sector limiter spanned a poloidal angle of about 50°. Both limiters, made of molybdenum, were 180° toroidally away from the arcing and erosion probes.

In case B the arcing source and the erosion probes were positioned 180° toroidally away from the collector probe. In addition, a further aperture limiter of titanium was installed, giving nearly a symmetric SOL-geometry between the locations of the source and the collector into both toroidal directions.

The surface normal of the Li-side of the erosion probe was parallel to the plasma current, whereas the Ag-side was antiparallel. Windows on the outside of the torus in the horizontal midplane allowed to photograph the plasma in the vicinity of the Ti-limiter and of the arcing source with and without time resolution.

The high speed movie camera Pentacon Pentazet 16 usually was

chosen to run at 1000 frames per second recording on ORWO-negative film NP 7 (ASA 400).
In all experiments the arcing source was positioned behind the wall at a minor radius of 115 mm. The radius of the molybdenum aperture limiter was 85 mm and that of the titanium one was 82 mm. The edge of the sector limiter was positioned at 75 mm. The erosion probes were inserted into the edge plasma up to a minor radius of 75 mm.

The Si-collector samples were mounted in a probe head of copper. This probe head was positioned up to a minor radius of 70 mm using a vacuum transfer system and was at floating potential. The collectors were exposed perpendicularly to the magnetic field lines facing the ion and electron drift direction (co- and counterdirection of the plasma current). The width of the collector probes was 12 mm and its length was 25 mm, giving the possibility to investigate radial dependences.

2.4. Experimental procedure

After baking the torus vessel at a temperature of 290° and a soft H_2-glow discharge cleaning procedure (460 V, 0.2 A/m^2) Ohmic hydrogen discharges were made with the following parameters: plasma current I_p = 10 kA, line averaged electron density $n_e = 2 \cdot 10^{19}$ m^{-3}, toroidal magnetic field B_T = 1.35 T, safety factor $q \approx 10$ and pulse length about 9 ms. In all cases reported here, the direction of the toroidal magnetic field was parallel to that of the plasma current.

After obtaining a stable regime with highly reproducible discharges, the collector probe was positioned at the exposure location. Due to gas desorption from the probe head the loop voltage was somewhat higher during the next two discharges but reached its original value eventually. After this conditioning of the collector probe, the metal impurities were injected by exposure the erosion probe into the edge plasma or by ignition of an arc between the Ta-cathode and the Cu-anode. In order to minimize the gas emission from the Ta-cathode, this system was preconditioned by preceding arc ignitions in vacuum.

The arc events during the tokamak discharges were recorded by taking photographs.
The impurities released by the arcing or erosion probes and transported by the plasma were collected on single-crystal silicon samples. In each configuration (A and B) six experiments were made with various numbers of discharges. After exposure, these samples and the limiters of Ti and Mo were analyzed by RBS, SIMS and AES. RBS was partly applied in channelling geometry to improve the sensitivity for the detection of the impurities and to measure the Si-damage for determining the hydrogen flux.

3. Results and discussion

3.1. Properties of the edge plasma without impurity injection

In order to study the influence of the impurity injection on the edge plasma behaviour, the collector probe was applied in normal discharges without impurity injection. Typical results of such an exposure are presented in fig. 4. This figure shows the damage amount of the Si-crystal induced by the edge plasma and the amount of collected impurities in dependence on the minor radius. It has to be noted that the particle fluxes were detected in the boundary layer on minor radii inside and outside the region shadowed by the limiters. A strong plasma decay with a decay length of a few mm was found to occur within the scrape-off plasma at minor radii between 90 and 95 mm /6/.

The damage amount contains information on the impinging hydrogen flux. At high fluences, as observed here /6/, saturation occurs and the proton impact energy can be derived. Ion energies between 60 eV and 150 eV have been estimated depending on the minor radius, the direction of the plasma flow and the magnitude of the discharge current.

A remarkable result is that the values of the damage amount and hence of the derived ion impact energy are larger in codirection of the plasma current than those in counterdirection inside the separatrix while the opposite is true in the SOL-plasma.

This indicates an asymmetric plasma flow to the collector probe, depending on the minor radius. The asymmetry inside the separatrix can be due to the toroidal electrical field which causes a directed motion of the plasma ions and electrons with the consequence that the sheath potential is differently influenced on both probe sides /6/.

After these shots without impurity injection only the expected intrinsic impurities Fe, Cr (wall material), Mo (limiter material) and also Cu were detected. The detected Cu indicates an erosion of the collector sample holder and a redeposition on the Si-samples. There are arguments that these effects do not influence the qualitative results of the collector probe measurements, derived below /6/. However, it cannot be ruled out that the observed radial dependences of the deposited impurity amount are somewhat affected by erosion and redeposition processes on the collector surface. Generally, the deposited amount of all impurities decreases with increasing minor radius with a decay length of a few cm in this region.

3.2. Response of the plasma to the impurity injection

Fig. 5a shows the temporal evolution of the plasma current I_p, the loop voltage U_L, the line averaged electron density n_e, and the radiated power P_r in a discharge with very strong impurity injection, initiated by an arc ignition at 3 ms. For comparison, their evolution is also shown without injection.

The injected metal impurities caused an increase of the radiated power P_r. The increase of the loop voltage U_L after the injection is due to both, an increase of Z_{eff} and a decrease of the electron temperature. Typically the signals of U_L and P_r developed two separated maxima. The first maximum occurred immediately after the arc ignition. The second appeared about 2 ms later. The first maximum is caused by the release and ionization of metal vapour from the Ta-cathode while the second peak can be explained by ablation of macroparticles which are released from the arcing source with temporal delay. Time resolved photographs taken from the plasma in the vicinity of

the arc source support this interpretation. Fig. 6 shows the light emission from the metal vapour at about 3 ms and the emission of the macroparticles at later times.

The changes of the signals of U_L and P_r caused by the arc vapour at 3 ms relax within a time of 1 ms, which is in the order of magnitude of the particle confinement time of CASTOR.

As can also be seen from fig. 5a the line averaged electron density rose by a factor of 2. This density increase can be associated with the amount of the injected metal impurities. However, the temporal behaviour of the density seems to be much more influenced by the macroparticles than by the cold arc vapour. In fact the increase of the line averaged density is mainly correlated to the emission of macroparticles (see fig. 5b).

This can be explained by the fact that the first rapid density change at 3 ms could not be detected by the interferometer. On the other hand it can be assumed that the radial profiles of the impurity concentration and the electron density which built up after the injection depend on the state of the injected material. With injection of a vapour cloud the major part is ionized in the boundary layer and only a minor part can penetrate into the core plasma. Hence the impurity confinement time is small and the electron density mainly increases in the boundary layer. As a result the line averaged density is less affected. On the other hand the screening action of the boundary layer on macroparticles is negligible. Most of them can penetrate into the core plasma and are ablated there. In this case the impurity confinement time is larger and the electron density increases in the core plasma which leads to a strong effect on the line averaged density . On the other hand the effect of the injected macroparticles on the mean electron temperature in the core plasma is small. It could be established that the change of this value is less than 10 % during the plateau phase with the exception of the phase immediately after the arc ignition (at 3 ms) where the determination of T_e is difficult. The plasma energy losses by ablation of the macroparticles, ionization of the impurity

atoms and enhanced radiation were largely compensated by an increased ohmic input power.

Effects of the impurity injection on the edge plasma are documented by the collector probe measurements. Fig. 7 reveals that the injection of the cold arc plasma and of the macroparticles influenced the plasma flux to the probe electron side, when the arcing source was arranged close to that side of the collector probe (configuration A). Using the correlation of the Si-damage to the ion impact energy and the electron temperature, an unusual radial T_e profile is found in the vicinity of the impurity source, T_e is found to decrease towards the plasma centre inside the separatrix, probably due to ablation and ionization processes. After injection the ion impact energy was estimated to be lower than 50 eV at a minor radius of 70 mm during the rest of the discharge, whereas it is about 100 eV without injection.

However, the plasma flux to the ion side of the collector probe does not seem to be affected. An influence on the plasma flux to both sides of the collector probe was also not observed when the arcing source was located further away from the collector probe (configuration B). This is an indication that the local impurity injection causes an instationary plasma phase with toroidal inhomogeneities of the plasma flow maintained in a time scale of milliseconds.

3.3. Motion of injected macroparticles

The macroparticles are ejected from the molten surfaces of the arcing source with temperatures of 3000 - 5000 K. The path of these droplets can be photographed because of their light emission or by the light emission of the ablating vapour cloud. The evaporation of the macroparticle is strongly forced by its interaction with the plasma. Although the photographs were taken without any selective filter there is evidence that in the present experiments the light emission of the vapour cloud was detected (see below).

Photographs taken with an exposure time somewhat longer than the duration of the discharge reveal a nearly isotropic emis-

sion from the source and a nonuniform motion of the macroparticles (see fig. 8). Obviously, the trajectory of most particles shown in fig. 8a is straightlined. These particles moved through the torus and were partly reflected at the wall. In another discharge, particles were dominant which could not reach the torus centre (fig. 8b). In particular the final path of these particles is not straightlined but shows that the particles were deflected into counterdirection of the plasma current. A more detailed picture of the different particle motion is obtained by time resolved photographs.

The example shown in fig. 9 demonstrates that particles could be emitted during and after the tokamak discharge. The emission speed of the particles derived from the path length and the exposure time changed with the time of emission. At first, during the discharge particles are ejected with velocities larger than 100 m/s and later, after the discharge, particles with a speed of some m/s were present. The track of the particles ejected after the discharge was always straightlined, whereas particles emitted during the discharge were often deflected, when they passed the boundary layer and penetrated into the central plasma and interacted with it. This plasma-particle interaction is indicated by an enhanced light emission due to a stronger ablation.

The deflection of the particles is not correlated with the plasma disturbance induced by the arc ignition. Photos taken in discharges without arc ignition show that dust particles removed from the wall and the limiters are much more deflected than particles produced by arcing (see fig. 10). This can be explained by their lower emission speed. Usually the release of dust particles occurred during the first high power discharges after installation of new limiters.

In order to find out the causes of the deflection of the macroparticles in the plasma the path curvatures can be taken into consideration. A characteristic feature of the deflection is their direction in counterdirection of the plasma current. The time scale of the acceleration process can be quite different. Generally, curved paths of macroparticles were observed as shown in fig. 6. In these cases an acceleration up to values of some 10^4 m/s^2 in a time of ms-range has to be assumed in order to explain these deflections. A more detailed evaluation of the curvatures reveals that the trajectories cannot be explained by a constant force.

In another discharge the macroparticles were suddenly deflected in a time scale shorter than 10^{-5} s (see fig. 11). At the time of the deflection an intensive ablation cloud was observed. Both facts together, the deflection and the enhanced ablation, indicate an anisotropic heat flux here, which caused an asymmetrical ablation with the consequence that the macroparticle was accelerated by repulsion forces. Probably such a sudden deflection is due to the impact of runaway electrons. Because the macroparticle is unshielded against the fast electrons, their energy is consumed for sublimation and transferred into kinetic energy of the released Ta-atoms. Assuming a sublimation energy h_S of about 3 eV and a mean kinetic energy of the ablating Ta-atoms $E_{kin} \approx 0{,}3$ eV, which corresponds to a sublimation temperature of about 3000 K, a fraction of 10 % of the received heat flux Q is transferred into kinetic energy of the released atoms.

The correlated heat flux necessary to explain the observed deflection can be roughly estimated taking into consideration the original momentum of the macroparticle.

Provided that the mass loss due to the sudden ablation did not change the mass of the macroparticle substantially, a 45^0-deflection is obtained if the momentum transferred to the macroparticle by the ablating atoms equals the original momentum of the macroparticle $M \cdot v_0$.

$$M \cdot v_0 = \dot{N} \Delta t \cdot m \cdot v$$

Here $\dot{N}$ is the ablation rate, $\dot{N} \Delta t$ the number of released Ta-atoms and $m \cdot v$ the momentum of a Ta-atom.

The number of the ablated Ta-atoms is obtained by

$$\dot{N} \Delta t \simeq Q/h_S$$

hence

$$Q \simeq h_S \cdot \frac{M \cdot v_o}{m \cdot v}$$

Taking a 1 µm-size particle with a speed of 100 m/s a heat flux of about 10^{21} eV/s·mm^2 is necessary to deflect heavily this particle in a time scale of 10^{-5} s.

It can be argued that the bended paths of the macroparticles are also due to repulsion forces.

In a tokamak plasma a macroparticle can be subjected to several forces /7/. However, a force into counterdirection of the plasma current can only be explained by the electrical field caused by the loop voltage and by momentum transfer of impinging particles or ablating atoms. The macropraticle can experience an electrical force because it is negatively charged and surrounded by a sheath similar to a floating probe. The acceleration by this force can be estimated knowing the charge of the particle. The sheath potential which builds up in front of a solid probe in a hydrogen plasma is about 3 kTe/e. If it is assumed that the scale length of the voltage drop is the Debye-length, the electrical field and via the radius of the macroparticle, the charge can be estimated as

$$q = 4\pi\varepsilon_o \cdot \Delta\tilde{\Phi} \cdot \frac{r_T^2}{r_D}$$

Here $\Delta\tilde{\Phi}$ is the potential drop, r_D the Debye-length, r_T the radius of the particle and q its charge.

With an electron temperature of 300 eV, a plasma density of 10^{19} m^{-3} and a loop voltage of 2.5 V, the acceleration a for Ta-particles is obtained as

$$a = 4 \cdot 10^{-8} \cdot \frac{1}{r_T} \qquad \text{in SI units.}$$

As can be seen the acceleration scales with the reciprocal radius of the particle. For typical values of this radius of about 1 µm the acceleration by the electrical field caused by the loop voltage is too small to explain the observed bended paths. Hence collisional or repulsive forces have to be assumed

to cause all observed deflections into counterdirection of the plasma current.

A momentum can be transferred to the macroparticle by the impinging plasma ions and by the ablating metal atoms. In both cases an anisotropic ion or heat flux to the macroparticle has to be assumed.Because of the acceleration of the ions and the deceleration of the electrons by the sheath potential and the lower mass of the electrons, the direct contribution of the electrons to the momentum transfer to the surface of the macroparticle is much smaller than that of the ions in a thermal plasma without runaway electrons, although the ions get a major part of their energy from the sheath which is maintained by the electron flow.

Neglecting at first the part of electrons to the heat flux the relative contribution of both atomic particle fluxes (the impinging ions and the ablating atoms) to the momentum transfer to the macroparticle depends on the energy of the impinging plasma ions.

Assuming a total absorption of the impinging ion energy at the macroparticle, and that 10 % of this energy is transferred into kinetic energy of the ablating atoms ($E_{kin}/h_s \approx 0.1$, see above), a simple relation can be derived for the ratio of the momentum transfer of the impinging ions to that of the ablating atoms.

$$\frac{\Delta p_H}{\Delta p_{Ta}} \approx \frac{v_{Ta}}{0,1\ v_H}$$

where Δp is the momentum transfer caused by the protons and the Ta-atoms and v is their corresponding velocity. Taking into consideration the ion acceleration by the sheath, with kT_e = 300 eV in the core plasma the momentum transfer by the ablating atoms is about 10^3 times larger than that of the impinging plasma ions. It demonstrates that the deflection of the macroparticles is due to an anisotropic ablation even if only atomic particle fluxes are considered. Hence the continuous deflection of the macroparticles is also an indication of a preferential heat flux into counterdirection of the plasma current in the core plasma.

Probably this preferential heat flux is correlated to an asymmetric electron flow. However, a more continuous distribution of nonthermal electrons in time and space has to be assumed here than in the case of the sudden deflection.
Such continuously bended path curvatures were also found in experiments with injection of fuelling pellets /8/. In this paper it has been proposed to use the path deflection as a diagnostic tool for determining the spatial distribution of nonthermal electrons.

Besides the path deflection of the macroparticles in counterdirection of the plasma current caused by repulsion forces of the ablating atoms, a deflection of the visible ablated vapour cloud was observed, too.
In particular, this effect clearly appears for the light emitting vapour cloud of macroparticles ejected after the tokamak discharge which have low speeds (see fig. 9), but it can also be observed for particles ejected during the tokamak discharges with a higher speed (see fig. 6c). The deflection is directed towards the bottom side of the torus and can be explained by the electron drift in the toroidal magnetic field.

Due to the temperature of several thousands Kelvin a macroparticle ejected by arcing emits atoms and electrons with a Maxwellian distribution. Obviously there are enough electrons which have the ability to excite ablated atoms whose deexcitation was observed by the emitted light. Thereby the macroparticle acquires quickly a positive charge, and the ablation cloud becomes negative.
The electrons of this cloud are guided by the magnetic field. The inhomogeneity of the torus field causes a drift of a negative charge toward the bottom side of the torus. Assuming a mean energy of the emitted electrons of 0.5 eV and a toroidal field of 1 T, the drift velocity is about 1 m/s. This value agrees well with the observation.

3.4. Transport of impurity ions

Properties of the transport of the injected impurity ions were studied by surface analysis of the deposited material on the collector probes and on parts of the limiters.

The propagation of the injected Ta-impurity in the vicinity of the source can be deduced from investigations of the limiters. Although the Ti-limiter was used during experiment B only, while the Mo-limiter was used during experiment A and B, this seems to be permissible because the injected Ta-amount was much larger with configuration B.

Fig. 12 shows the experimental configuration and the radial dependence of the collected amount of Ta on both sides of the limiters. The decrease of the collected Ta-amount on the Mo-limiter with decreasing minor radius near the plasma is probably due to erosion effects. Evidence of this erosion is given by the detected Mo-fluxes on the collector probe. Fluxes of Ti, the other limiter material could not be detected which indicates that erosion at radii larger than 82 mm is negligible.

Comparing the deposited amount of Ta on the different sides of both limiters at minor radii larger than 82 mm the following qualitative results are obtained:

- On all limiter sides the injected impurity is detectable.
- On the side which faced the source more Ta was deposited than on the opposite side of both limiters.
- On the Ti-limiter more Ta was deposited than on the Mo-limiter.

The preferred transport of the injected material toward the Ti-limiter can be due to the ablation of the macroparticles deflected into counterdirection of the plasma current. This means the transport properties of the injected material along short distances are dominated by the transport of the macroparticles.

Typical results of the collector probe measurements are shown in fig. 13. With configuration A, the injected Ta was predominantly detectable on the electron side of the collector probe. This is not surprising and similar to the results found for the limiters because this side faced the Ta-source in a relative small distance of about 30 cm. The larger Cu-deposition on the electron side is a peculiarity of this experiment and is due to an additional Cu-flux from the arcing source induced by

arcing on the cathode holder. This was verified by arcing traces on the holder.

It should be noted that only impurity atoms released from the arcing source which were ionized and transported by the plasma could reach the collector probe because the source was behind the wall and had no line of sight connection to the collector probe. In a separate experiment it was checked that detectable amounts of Ta could not reach the collector probe without a tokamak discharge.

The toroidal asymmetry of the deposition of the injected material changed when the collector probe was located further away from the source. With configuration B, where both sources, the arcing source and the erosion probe, were 180° toroidally away from the collector probe, larger atomic fluxes of the injected Ta and Li[1)] were detected on the ion side of the collector probe. Such a behaviour was always found with Mo which was released from the limiter 140 degree toroidally away from the ion side of the collector probe. This leads to the conclusion that the flow of the impurities in the toroidal directions is nonsymmetric as found for the plasma flow. There is a preferred transport of plasma and impurity ions in codirection of the plasma current in the boundary layer. Comparing the absolute amounts of the collected Ta-impurity on both sides of the collector probe the Ta-flux into codirection is about 20 % higher than into counterdirection of the plasma current. For the limiter material the asymmetry was found to be even higher. This can be due to the fact that the asymmetry of the atomic Ta-transport is partly compensated by the deflection of the ablating Ta-macroparticles.

The small difference of the distance of the sources of Mo and Ta from the collector probe does not seem to have a significant influence as documented by the rough results obtained on the dependence of the impurity detection probability on the

1) Ag from the erosion probe could never be detected, because of a negligible erosion of the Ag-layers. The latter fact was checked by RBS-Measurements of these layers before and after the plasma exposures.

toroidal distance between the source and the collectors. These results can be deduced from a comparison of the detected Ta-amounts on the limiters which were in the vicinity of the source and those on the collector samples which were 180° toroidally away. In spite of the large difference of the distance from the source the deposited Ta-amounts on the Mo-limiter and all collector samples exposed with configuration B are similar (compare also fig. 12 and fig. 13b).

Another explanation of differently pronounced asymmetries of the impurity fluxes could be a dependence of the toroidal transport on the atomic mass. This hypothesis is supported by the asymmetry of the detected Li-fluxes (fig. 13b) which is even larger than that of Mo. But this has to be proved in further experiments.

The wall material Fe, Cr did not show a definite behaviour. In most cases there is a nearly symmetric flow of Fe and Cr to the collector probe. The specific deposition behaviour of the wall material should depend on the location of the sources. However, comparing fig. 7 and fig. 13 it can be established that the transport behaviour of all intrinsic impurities was not strongly affected by the injection.

Discharges performed after these injection experiments showed a normal plasma behaviour without any peculiarity. Fluxes of the impurities injected before could not be detected in the subsequent discharges which shows that recycling effects were negligible.

4. Summary

The measurements with and without impurity injection have shown, that

- there is a nonsymmetric plasma flow to the collector probe. The preferred direction of this flow changes with the minor radius and is parallel to the codirection of the plasma current in near plasma regions of the boundary layer whereas it is in the counterdirection near the wall.

Controlled impurity injection by arcing and erosion probes into the plasma of the CASTOR-tokamak has demonstrated that

- a local injection can cause toroidal inhomogeneities of the plasma flow at least in the boundary layer in a time-scale of milliseconds,
- the plasma core seems to be much more influenced by injected macroparticles than by injected vapour due to the different screening action of the boundary layer in both cases,
- there exists an anisotropic component of the heat flux in the core plasma which causes a deflection of injected macroparticles into counterdirection of the plasma current by an anisotropic ablation. This heat flux may be attributed to nonthermal electrons,
- the short distance transport of the injected material is dominated by the transport of the macroparticles,
- the detection of atomic impurity fluxes does not seem to depend strongly on the toroidal distance between the source and the collecting surface,
- the long distance transport of atomic impurity fluxes has an anisotropic component into codirection of the plasma current.

Experiments carried out without controlled impurity injection have shown that the observed effects of the anisotropic plasma and impurity flow as well as the deflection of the macroparticles are not correlated to the plasma disturbance induced by the impurity injection. Nevertheless the aim of further experiments is to reduce the plasma disturbance by the impurity injection. The sensitivity of the used detection methods allows a considerable lowering of the injected impurity amount.

References

/1/ G.M. Cracken, P.E. Stott; Nucl. Fusion 19 (1979) 889

/2/ D. Hildebrandt et al.; Nucl. Fusion 25 (1985) 1745

/3/ D. Hildebrandt et al.; VII. PSI-Conference, Princeton 1986, to be published in J.Nucl.Mater.

/4/ CASTOR-tokamak group IPPCZ-256 (1985) Research Report

/5/ To be published as ZIE-Preprint

/6/ D. Hildebrandt et al.; submitted to Contrib. to Plasma Phys.

/7/ T. Ohkawa, General Atomic Report GA-A14232 (1976) San Diego

/8/ V. Anderson, ECA "12th Europ. Conf. on Controlled Fusion and Plasma Physics" Vol. 9F, Part II, 648, Budapest 1985

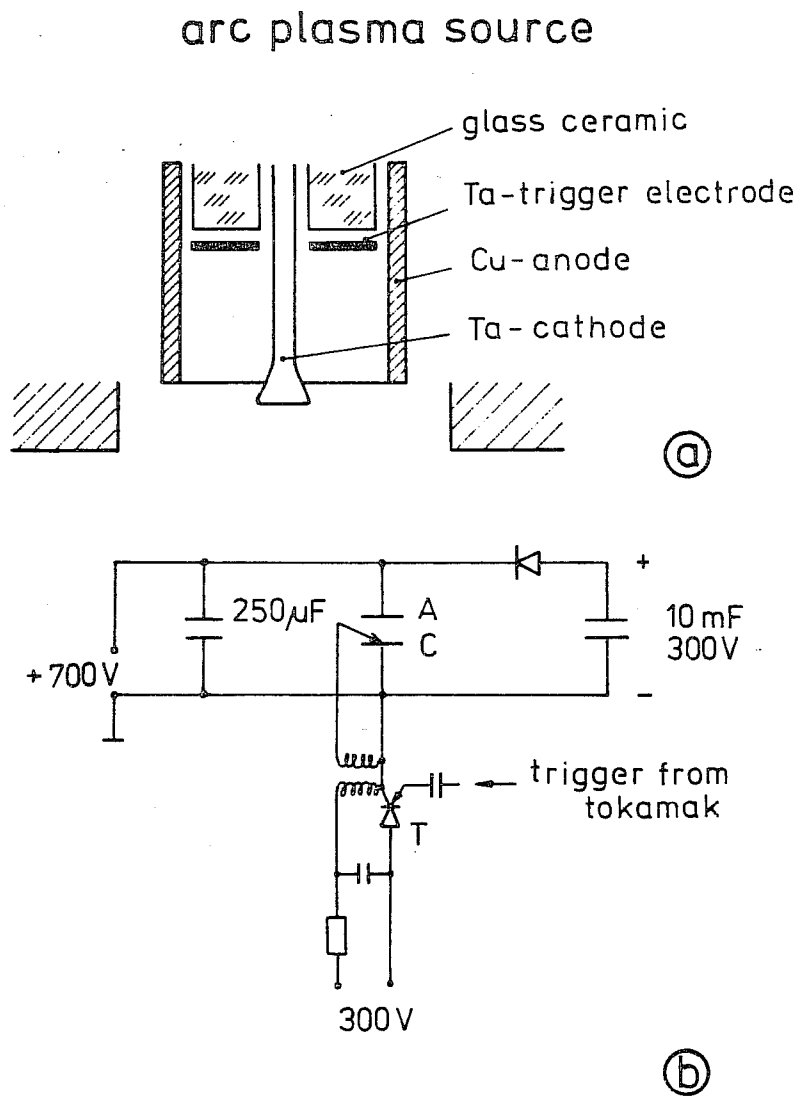

Fig. 1a: Arc plasma source.
A - anode, C - cathode, T- thyristor

Fig. 1b: Scheme of electrical circuit of the arc plasma source

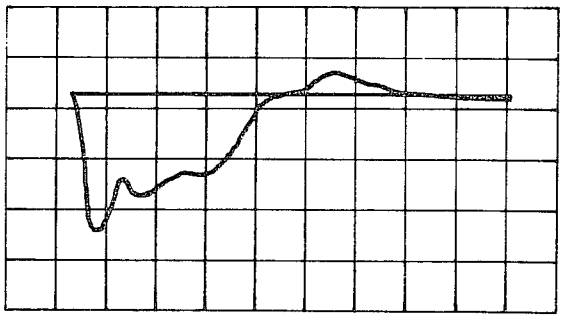

Fig. 2: Characteristic evolution of the arc current of the arc plasma source; 200 µs/div. and 4 kA/div.

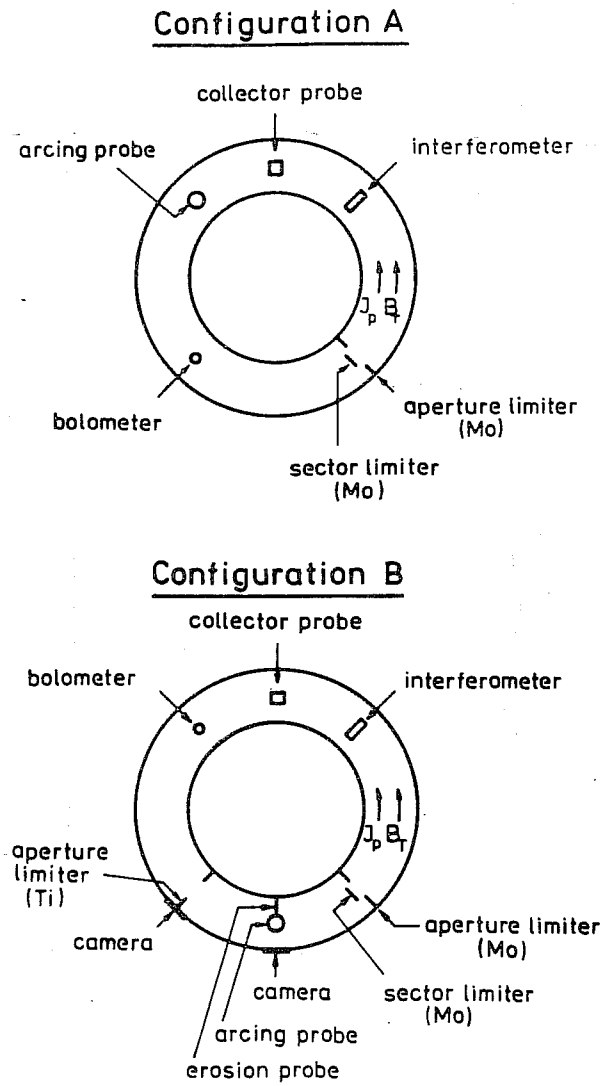

Fig. 3: The different experimental configurations.
I_p - plasma current, B_T - toroidal magnetic field

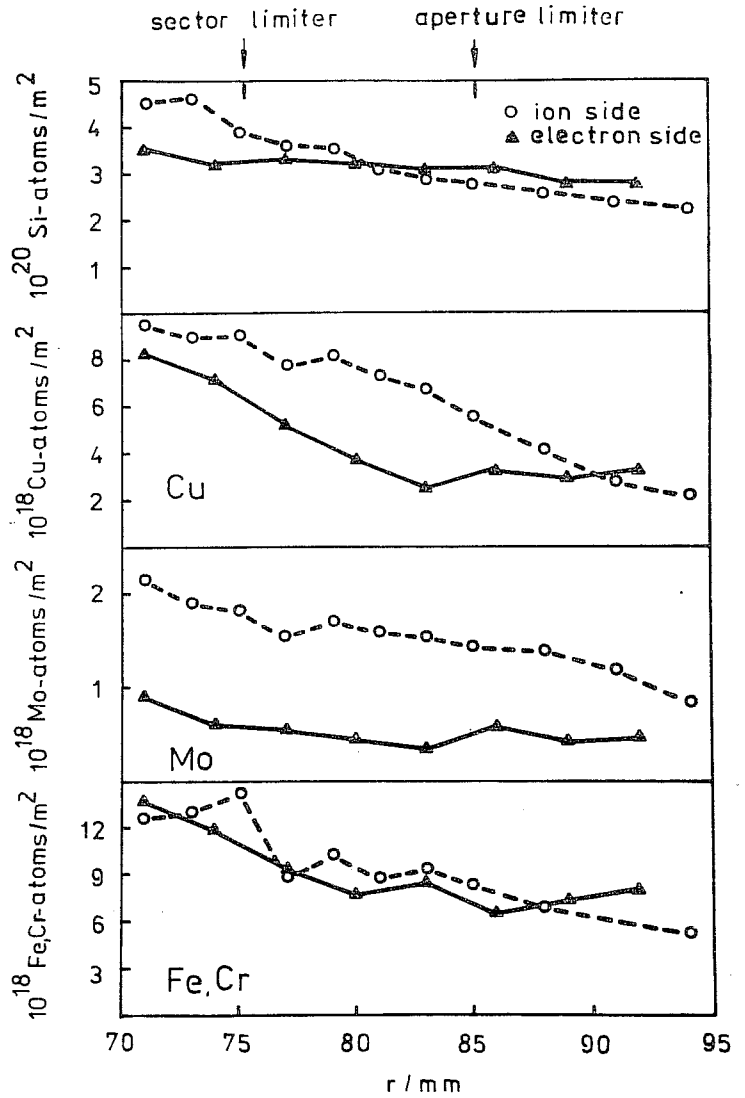

Fig. 4: Radial dependences of the damage amount of Si-samples and the collected impurity amounts in discharges without impurity injection.
Discharges 9850 - 9903

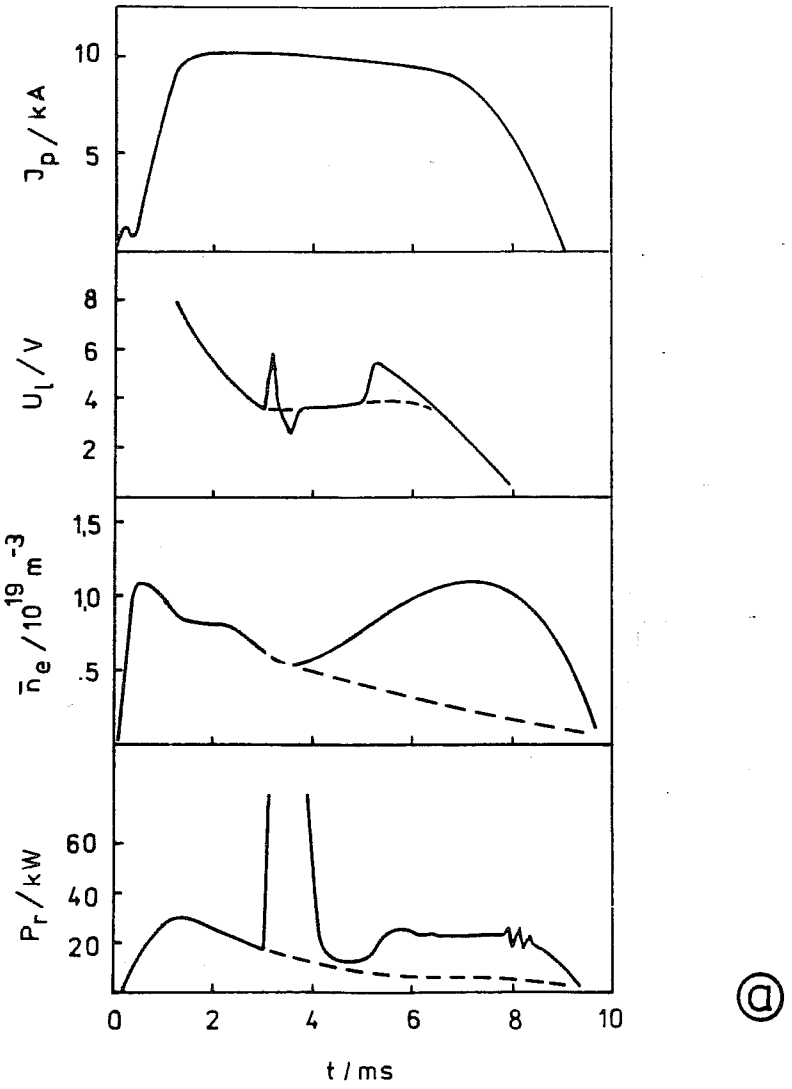

Fig. 5a: Temporal evolution of plasma current I_p, loop voltage U_l, electron density n_e and radiated power P_r in a discharge with strong impurity injection at 3 ms. Dashed curves: without injection.

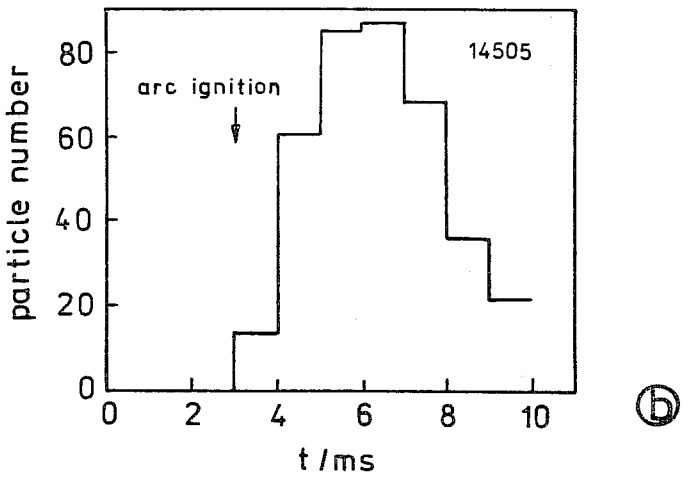

Fig. 5b: Number of macroparticles ejected by arcing as observed on the photographs at different times.

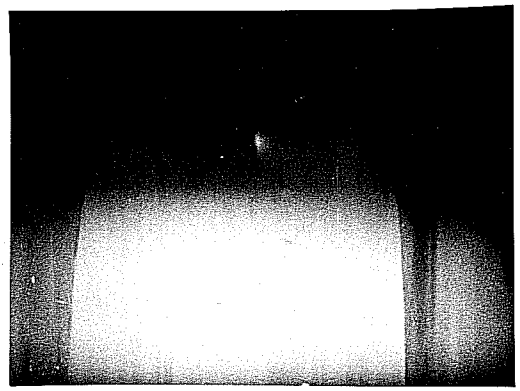

a

1-2 ms

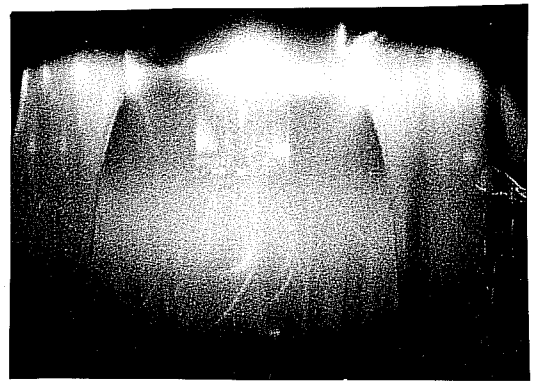

b

3-4 ms

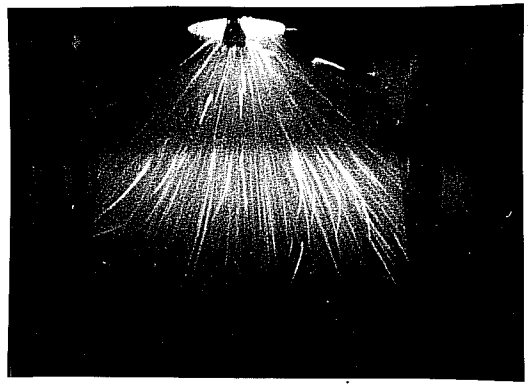

c

5-6 ms

Fig. 6: Photographs taken during different phases of a discharge with impurity injection by arcing at 3 ms. Shot-No. 14505

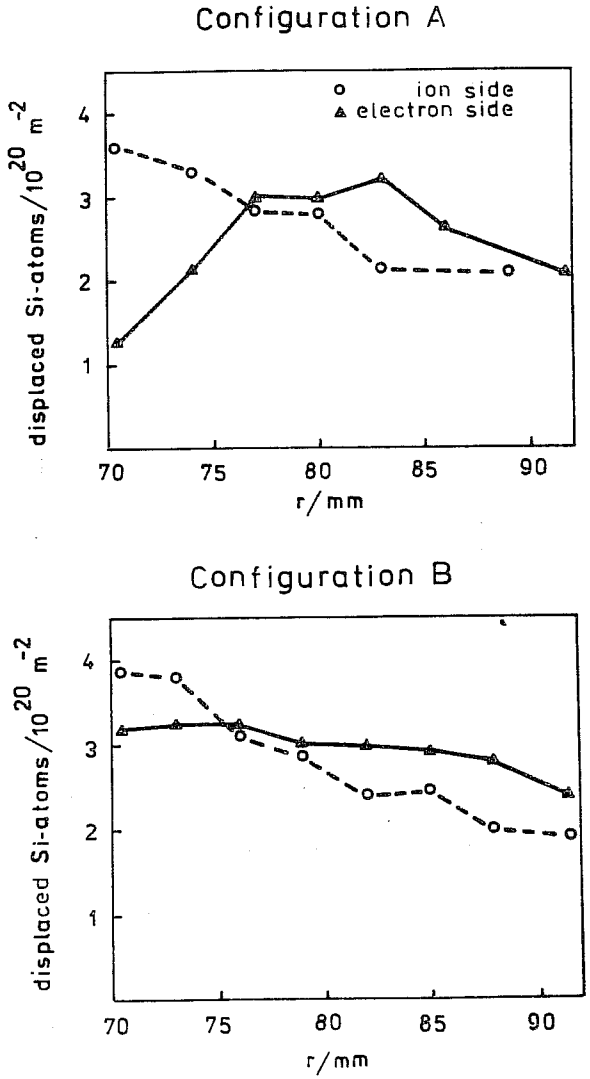

Fig. 7: Radial dependences of the damage amount of Si-samples exposed to discharges with impurity injection

Configuration A - discharges 14290 - 14297 and
Configuration B - discharges 14439 - 14471

a

b

Fig. 8: Photographs taken without time resolution (open shutter) during discharges with impurity injection in the vicinity of the arc source

a) discharge 14448 b) discharge 14456

2-4 ms

a

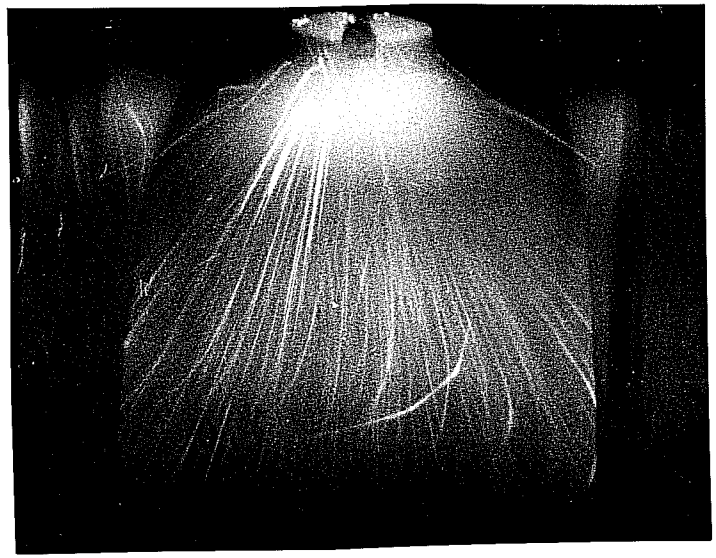

4-6 ms

b

Fig. 9: Photographs taken at different times after arc ignition showing the macroparticle emission during and after the tokamak discharge and the path of these particles; discharge 14461

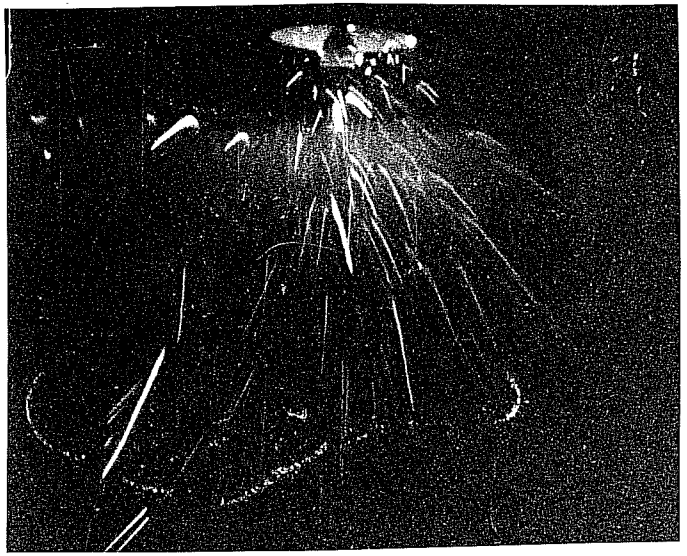

8-10 ms

c

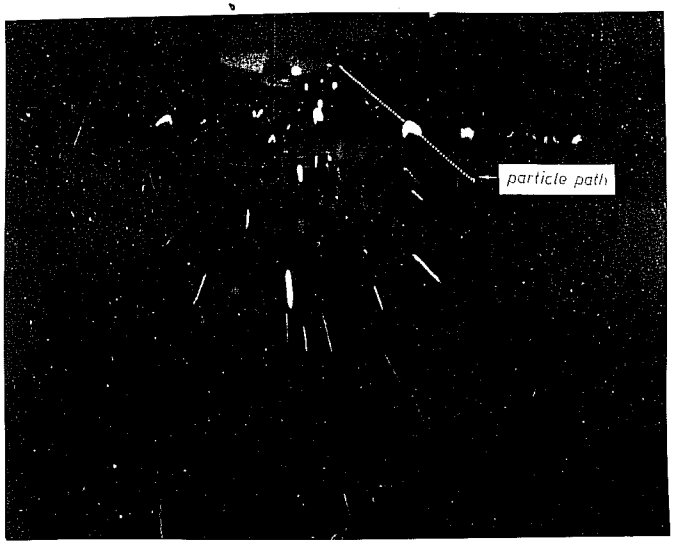

16-18 ms

d

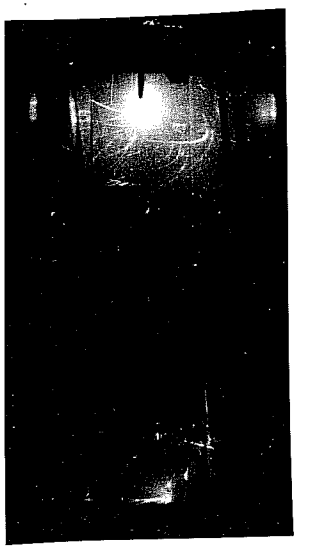

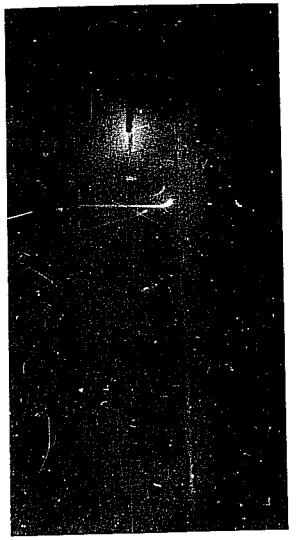

Fig. 10: Photograph of the plasma in the vicinity of the limiter showing the path of macroparticles released from the wall.

Fig. 11: Photograph showing a sudden path of macroparticles ejected by arcing at a time between 6 and 8 ms after current rise of the tokamak discharge; discharge 14461

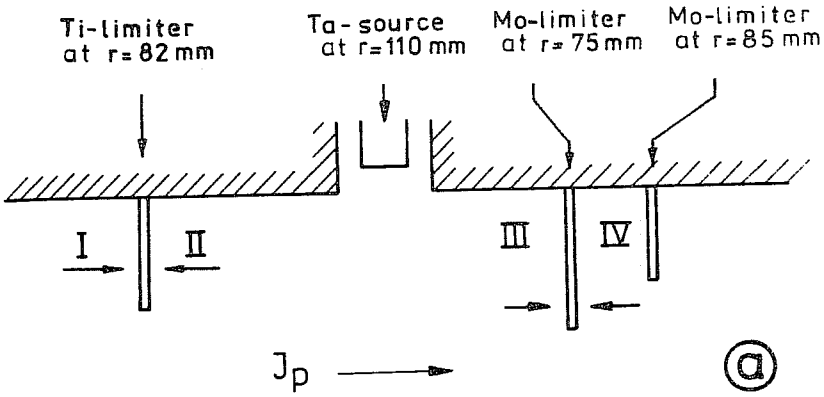

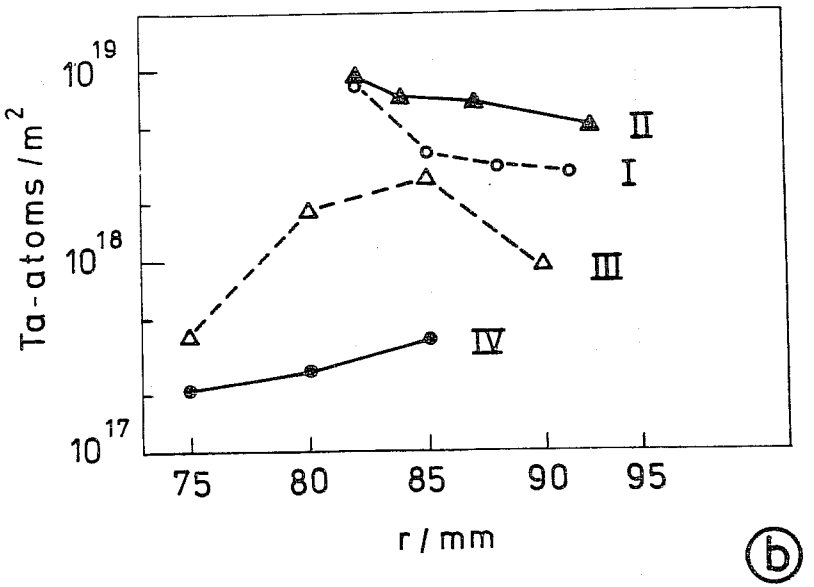

Fig. 12a: Location of the arc source and the investigated limiters (configuration B)

Fig. 12b: Radial dependence on the collected Ta-amount on the different surfaces of the limiters. Labels I-IV correspond to the surface as indicated in figure 12a.

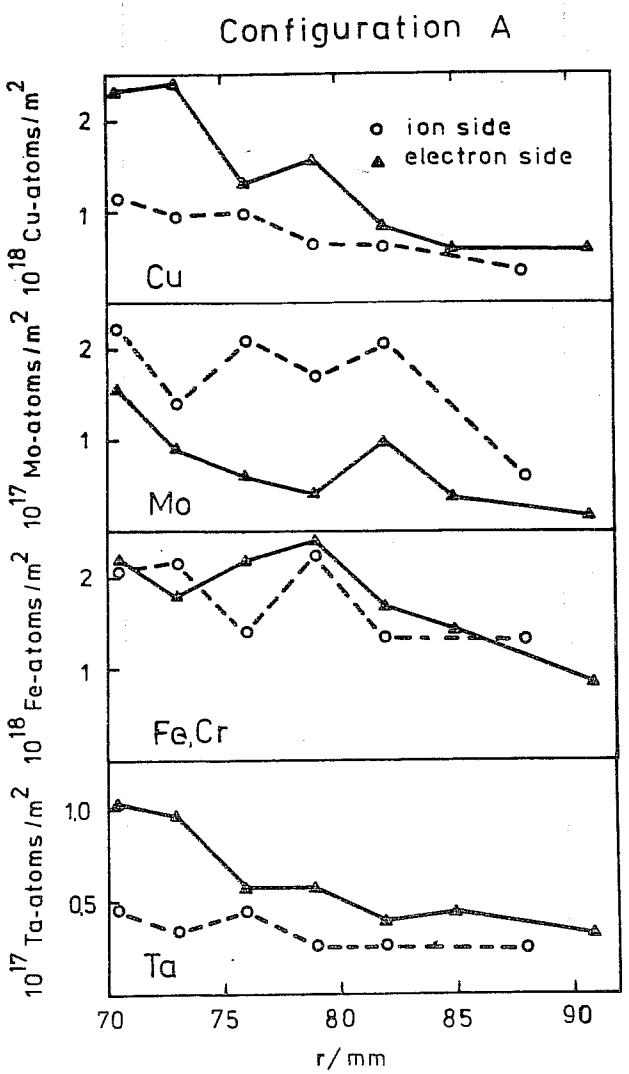

Fig. 13: Radial dependence of the collected amount of intrinsic and injected impurities.

a - Configuration A - discharge 14290 - 14297

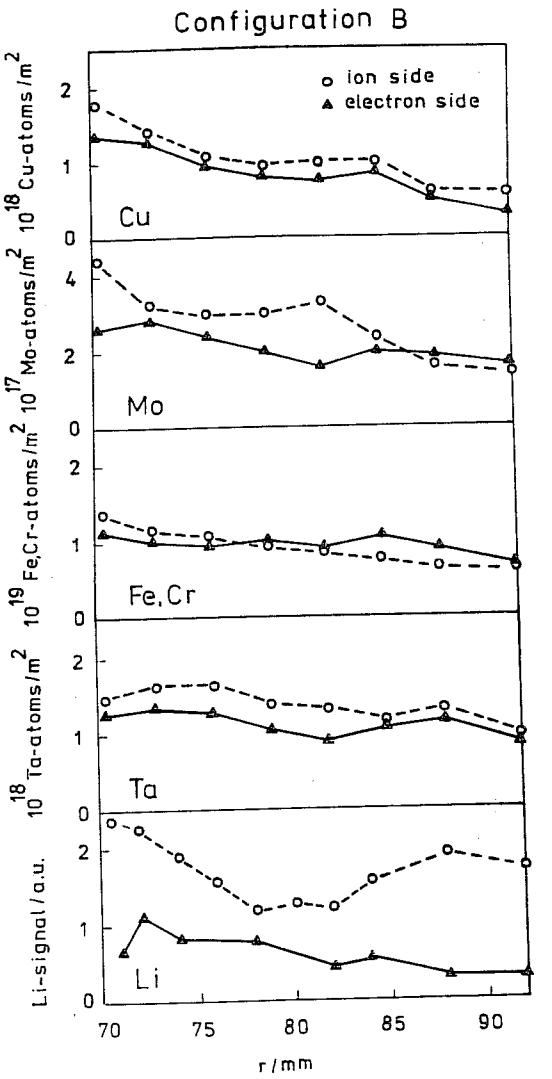

Fig. 13: Radial dependence of the collected amount of intrin sic and injected impurities.

b - Configuration B - discharge 14439 - 14471